

Novel electromechanical actuation based on spongy graphene paper

Ying Hu,^a Tian Lan,^a Guan Wu,^a Zicai Zhu,^a Xiaomin Tao^b and Wei Chen^{*a}

Electronic Supplementary Information (ESI) available:

Experimental description:

Materials: Natural graphite flake (325 meshes, 99.8%, ABCR GmbH & Co. KG) was obtained from Sigma Aldrich. Phosphorous oxide (purity 98 %) and potassium peroxydisulfate (purity 97%) was obtained from Alfa Aesar. HI acid was supplied by Sinopharm Chemical Reagent Co. and used as received. All other chemicals were obtained from Sinopharm Chemical Reagent Co., Ltd and 18 M Ω Milli-Q water was used in all experiments.

Preparation of RGO paper: GO was synthesized from natural graphite flake (325 mesh, 99.8%, ABCR GmbH & Co. KG) according to a modified Hummers method and has been described in our previous publications.¹⁻³ GO paper was fabricated by dropping aqueous GO dispersions onto the glass slide followed by drying in an oven at 60 °C. The reduction was carried out by immersing GO paper into HI acid solution for 10 min. After that, the RGO paper was repeatedly rinsed with ethanol to remove residual HI acid and dried at 40 °C.

Fabrication of U-shape sG actuator: The RGO paper was cut into the strip shape with dimension of 27mm \times 7mm \times 5 μ m (length \times width \times thickness), and the 22mm \times 1mm (length \times width)-middle part was cut off from the strips to shape into a

U-shape actuator. After that, a voltage of 10V was applied on the U-shape actuators to fabricate the sG actuator.

Measurement of the actuation: For actuation measurement, the U-shape actuators were connected to the electrode with the two ends to form electric circuit. The laser displacement sensor (LK-G80, Keyence) and infrared thermometer were employed to measure displacement and temperature change of the U-shape actuator under the input voltage. For the sG and RGO paper actuators, the laser displacement sensor was placed under the actuator to record the upward and downward displacement (figure 2a). In addition, for the thickness displacement measurement, the sG paper strip with the dimension of 10mm × 2.5mm (length × width) was fixed on the glass substrate with two ends connected to the electrodes, similar with the configuration shown in figure 2d. The laser displacement sensor was located over the strip to record the displacement change along the thickness direction in response to the electric and infrared lamp stimuli.

Characterization: GWINSTEK PSM-3004 programmable power supply and CHI600C electrochemical work station were used for providing direct voltage and alternating voltage, respectively. Digital infrared lamp purchased from Nanjing ZhongJingKeYi technology co.,LTD was employing for direct heating. Scanning electron microscopy (SEM) images were performed with Hitach S-4800 filed emission scanning electron microscope. X-ray diffraction (XRD) patterns were obtained on X'Pert-Pro MPD (Cu-Ka). Raman spectra were collected using a Jobin-Yvon LabRam HR 800 confocal micro-Raman system equipped with an electrical-

cooled detector. The excitation wavelengths were 632.8 nm with a He-Ne laser. The CTE was measured under Ar gas by thermomechanical analysis (EXSTRA TMA/SS7100) with a preload of 5mN and a temperature ramp rate of 5°C/min.

Figure S1 displays the optical images of the GO paper as well as RGO paper with reduction time of 10 min. We could see that GO paper display a brown color (left image) while the RGO paper shows a shiny metallic luster (right image), with an increased electrical conductivity of about 210 S/cm and excellent flexibility. After the formation of sG paper, its electrical conductance is increased compared with that of the RGO paper.

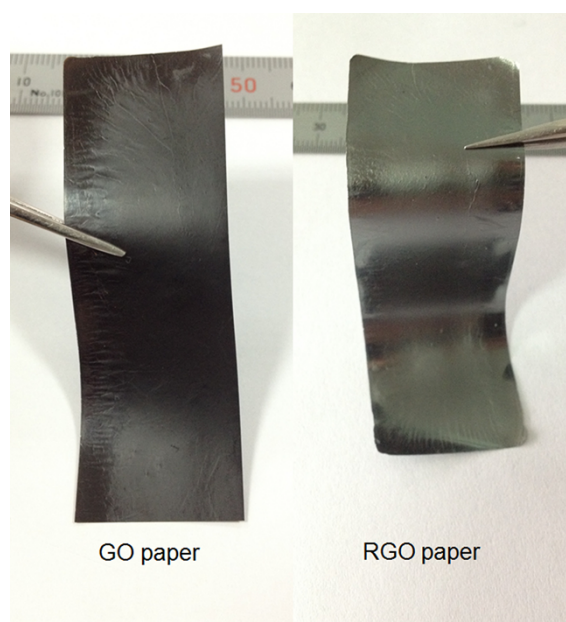


Figure S1. Optical images of GO paper (left) and RGO paper (right).

Figure S2 shows the comparison of XRD spectra for the GO and RGO paper as well as sG paper. It can be seen in figure S2a that the interlayer spacing of the RGO paper

is decreased from 8.1Å ($2\theta = 10.9^\circ$) for original GO paper to 3.7Å ($2\theta = 24^\circ$). Meanwhile, the peak at 10.9° decreases but not disappear for the RGO paper, revealing there still remains unreduced oxygen containing functional groups after the reduction process. The HI acid reducing process is conducted from outer of the GO paper to its inner. Therefore, the inner part of the GO paper is not fully reduced because of the short reduction time. In contrast to the RGO paper, the XRD peak at 10.9° totally disappears for the sG paper, indicating the effect of thermal reduction of the oxygen containing functional groups in the fabrication of sG paper.^{4,5}

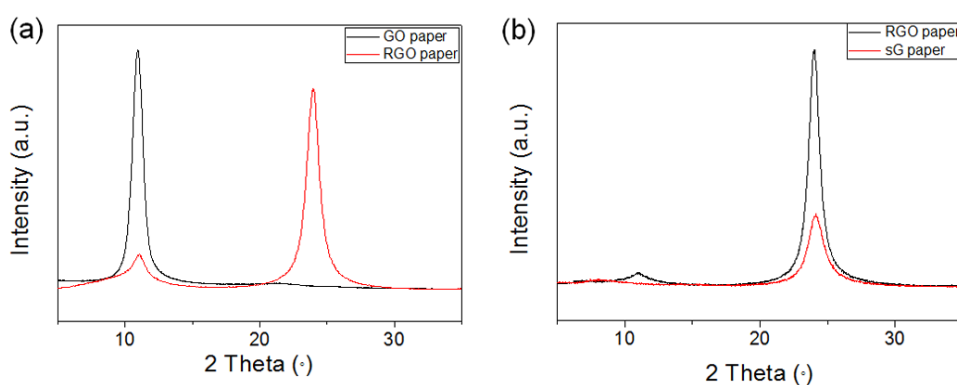


Figure S2. (a) XRD patterns of the GO paper and RGO paper. (b) XRD patterns of RGO paper and subsequently fabricated sG paper.

Figure S3 shows Raman spectra of GO paper, RGO paper, and sG paper by applying 10V voltage. The D peak ($\sim 1332\text{cm}^{-1}$) as well as G peak ($\sim 1591\text{cm}^{-1}$) are clearly observed. With the increase of the reduction degree, the peak intensity ratio of the D peak to the G peak (I_D/I_G) is increased from GO paper to RGO paper and sG.^{6,7}

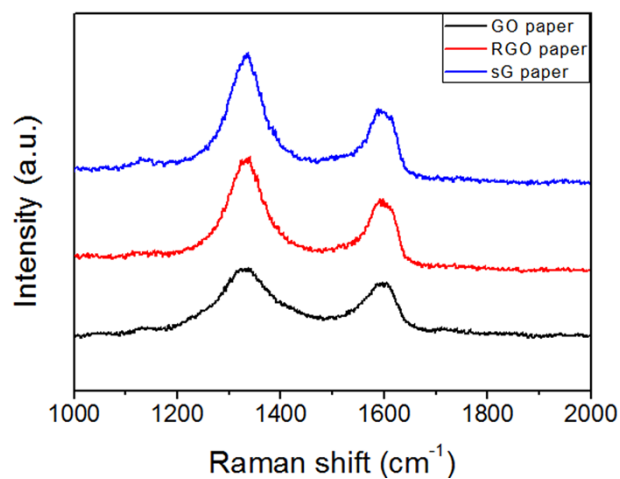


Figure S3. Raman spectra of the GO paper, RGO paper and sG paper.

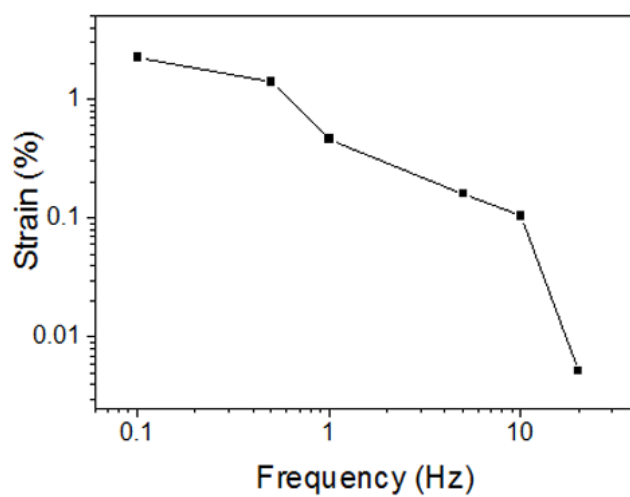


Figure S4. Actuation strain of sG paper as a function of frequency of the applied 10V square voltage.

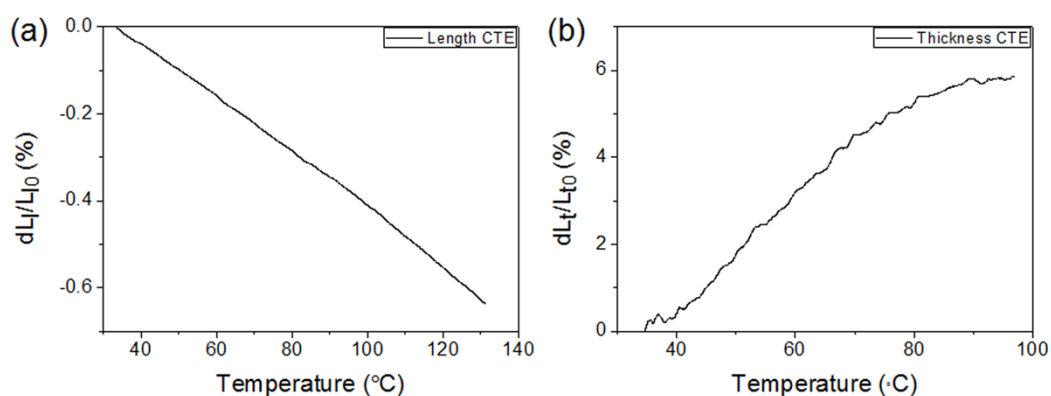


Figure S5. Thermal expansion curves of the sG paper along its length direction (a) and thickness direction (b) measured by TMA with a preload of 5mN.

In order to verify the effect of the gas molecules on the electric actuation, the electric actuation of sG paper both in air and in vacuum are all studied, as shown in figure S6. The vacuum test is conducted in a vacuum dry oven with the relative air pressure of about $-100 \times \text{kPa}$ and the electric actuation is simultaneously recorded by a digital camera. For the purpose of better observing the actuation, a strip configuration is adopted, in which a suspended strip shape sG paper with two ends fixed on the electrodes is connected to an electrical power (figure S6a). Figure S6b shows the electric actuation of sG paper in air. When applying 0.1Hz 5V voltage on the sG strip, it quickly shrinks with the voltage on, and recovers immediately with the voltage off. For comparison, the electric actuation of this sG paper under the same voltage in vacuum is also shown in figure 6Sc. Upon voltage, the electric actuation of the sG strip in vacuum is very small and can't be clearly observed compared with that of actuation in air. Moreover, the deformation of the sG strip under the different air

pressure is also presented, as shown in figure S6d. The experiment is conducted without the electrical stimulation. It can be seen clearly that the sG strip contract along the length direction in vacuum. Its thickness expansion in vacuum can also be observed in the inset magnified images in figure S6d. The deformation of sG strip in vacuum reveals the existence of the gas sealed inside the corrugated structure cavities in the sG paper. In vacuum, the pressure differences between inside and outside causes the deformation of the corrugated structures, thus the deformation of the whole sG strip. These results further confirm the influence of interlayer gas on the electric actuation of the sG paper.

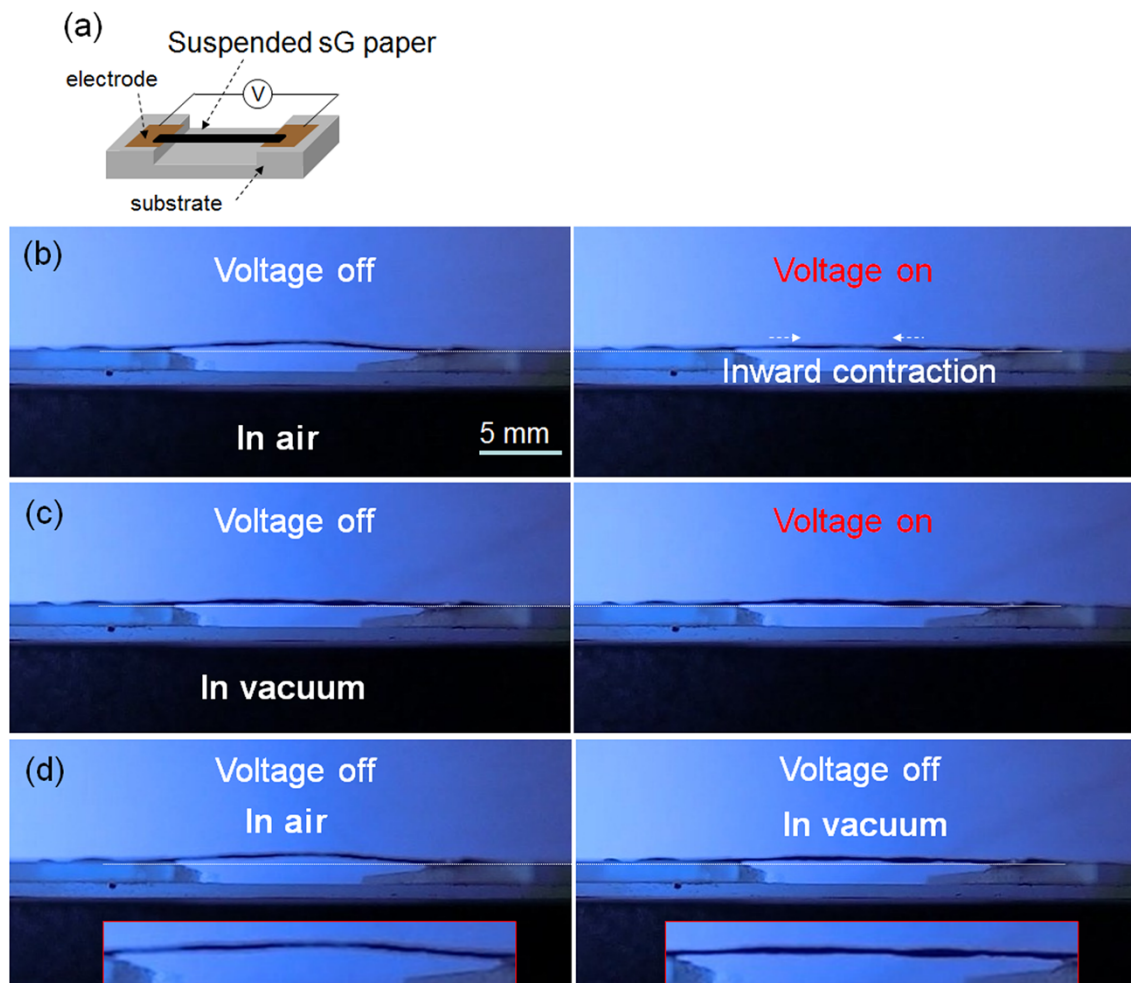


Figure S6. (a) Schematic illustration of the suspended sG paper strip upon electric stimulation. (b-c) Side view optical images of the suspended sG strip with the 0.1Hz 5V voltage off and on both in air (b) and in vacuum (c). Electric induced length contraction of the sG strip can be clearly observed in air.(d) Optical images of the suspended sG strip in air as well as in vacuum without voltage stimulation. The inset images in the red rectangles are the magnification of the suspended sG paper.

References

- 1 N. I. Kovtyukhova, P. J. Ollivier, B. R. Martin, T. E. Mallouk, S. A. Chizhik, E. V. Buzaneva and A. D. Gorchinskiy, *Chem. Mater.*, **1999**, 11, 771.
- 2 J. Liu, Z. Wang, L. Liu and W. Chen, *Phys. Chem. Chem. Phys.*, **2011**, 7, 13216.
- 3 Y. Hu, L. Lu, J. Liu and W. Chen, *J. Mater. Chem.*, **2012**, 22, 11994.
- 4 D. Krishnan, F. Kim, J. Luo, R. Cruz-Silva, L. J. Cote, H. D. Jang, J. Huang, *Nano Today* **2012**, 7, 137.
- 5 F. Kim, J. Luo, R. Cruz-Silva, L. J. Cote, K. Sohn, J. Huang, *Adv. Func. Mater.* **2010**, 20, 2867.
- 6 A. C. Ferrari and J. Robertson, *Phys. Rev. B*, **2000**, 61, 14095.
- 7 S. Pei, J. Zhao, J. Du, W. Ren and H. Cheng, *Carbon*, **2010**, 48, 4466.